Face Pose Tracking under Arbitrary Illumination Changes

Ahmed Rekik[1], Achraf Ben-Hamadou[2] and Walid Mahdi[1]
[1]*Sfax University, Multimedia InfoRmation systems and Advanced Computing Laboratory (MIRACL)*
Pôle Technologique de Sfax, route de Tunis Km 10, BP 242, 3021 Sfax, Tunisia
[2] *Total Immersion SA, R&D department, 26 Avenue du Général Charles de Gaulle, 92150 Suresnes, France*

Keywords: 3D Face Tracking, RGB-D Cameras, Lighting Condition Changes, Augmented Reality, Human Computer Interaction.

Abstract: This paper presents a new method for 3D face pose tracking in arbitrary illumination change conditions using color image and depth data acquired by RGB-D cameras (e.g., Microsoft Kinect, Asus Xtion Pro Live, *etc.*). The method is based on an optimization process of an objective function combining photometric and geometric energy. The geometric energy is computed from depth data while the photometric energy is computed at each frame by comparing the current face texture to its corresponding in the reference face texture defined in the first frame. To handle the effect of changing lighting condition, we use a facial illumination model in order to solve which lighting variations has to be applied to the current face texture making it as close as possible to the reference texture. We demonstrate the accuracy and the robustness of our method in normal lighting conditions by performing a set of experiments on the Biwi Kinect head pose database. Moreover, the robustness to illumination changes is evaluated using a set of sequences for different persons recorded in severe lighting condition changes. These experiments show that our method is robust and precise under both normal and severe lighting conditions.

1 INTRODUCTION

Face 3D pose tracking is an important topic for several research domains such as Human-computer interaction, augmented reality, *etc.* (Yin et al., 2006). These very last years, the research in this topic has dramatically increased (Fanelli et al., 2013; Padeleris et al., 2012; Cai et al., 2010). This arises particularly from the ubiquity of vision systems in our day life (i.e., webcams in laptops, smart-phones, etc.) and, recently, from the availability of low-cost RGB-D cameras, such as Asus Xtion Pro Live and Microsoft Kinect. The literature contains several works on face pose estimation and tracking (see (Murphy-Chutorian and Trivedi, 2009) for a survey). Since lighting conditions are rarely constant, the accuracy of the methods using 2D images are very sensitive to illumination changes. To solve this problem, Zhou *et al.*. (Zhou et al., 2004) impose a rank constraint on shape and albedo for the face class to separate the two from illumination using a factorization approach. Integrability and face symmetry constraints are employed to fully recover the class specific albedos and surface normals. Some recent works like (Fanelli et al., 2013; Padeleris et al., 2012) use depth images, but this solution is incomplete since depth data are also noisy for low-cost RGB-D cameras and the solution is to use both depth and color images to perform the tracking (Baltrušaitis et al., 2012; Rekik et al., 2013).

In addition to the combination of color and depth images, we propose in this paper a new 3D face tracking method that takes in account lighting condition changes. Our method uses a generic illumination model and does not require to characterise the light sources (*e.g.,* number, power, pose). The rest of the paper is organized as follows. In the first section, we describe the input data acquired from RGB-D camera. Section 3 details the proposed tracking method where first we present the general framework, then, we describe the illumination changes model. Finally, Section 4, details the experiments and results to evaluate the tracking accuracy of our method and its robustness against arbitrary illumination changes.

2 INPUT DATA DESCRIPTION

In this work, we have used a Kinect sensor as a RGB-D camera. Its depth sensor is a composed device con-

Rekik A., Ben-Hamadou A. and Mahdi W..
Face Pose Tracking under Arbitrary Illumination Changes.
DOI: 10.5220/0004686705700575
In *Proceedings of the 9th International Conference on Computer Vision Theory and Applications* (VISAPP-2014), pages 570-575
ISBN: 978-989-758-009-3

sisting of an IR projector of a point pattern (point structured-light) and IR camera surrounding the color camera, which are used to triangulate points in space leading to a depth map (Ben-Hamadou et al., 2010; Ben-Hamadou et al., 2013; Smisek et al., 2013). As illustrated in Figure 1, one can compute the 3D point cloud corresponding to the depth map pixels using the calibration parameters of the IR camera. Also, each 3D point can be projected in the color image using the calibration parameters of the color camera. In this way, we have all transformations to map data between 3D space, color image, and depth map. For the rest of this paper we assume that all the calibration parameters of the RGB-D sensors are known.

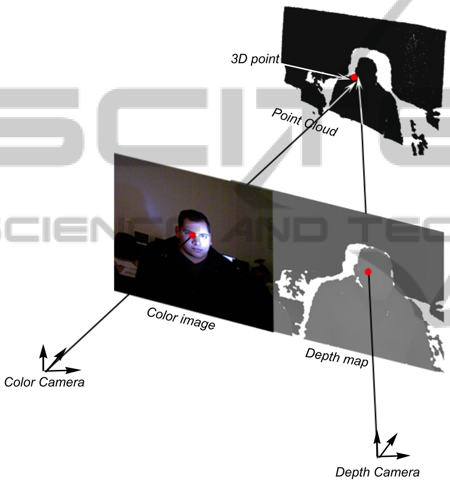

Figure 1: Illustration of the RGB-D camera geometry.

3 FACE POSE TRACKING METHOD

The 3D face tracking can be seen as an optimization problem where the goal is to find the optimal 3D rigid motion of the face between two consecutive acquisitions. In this process, we denote the optimal face pose as $\widehat{x}_t$ in the instant t, where $\widehat{x}_t \in \mathbb{R}^6$ involves the 6 DOF (*i.e.,* 3 translations and 3 rotation angles) of a 3D rigid motion. For each acquisition, the estimation of the face pose is an iterative process witch ameliorate an incremental estimation $\widetilde{x}_t$ until reaching the optimal estimation $\widehat{x}_t$. Initially, $\widetilde{x}_t$ is set to $\widehat{x}_{t-1}$ (*i.e.,* tracking result of the previous frame). Reaching the optimal estimation consist of minimizing an objective function f_{obj} measuring the distance between the *reference model* M^* and the *appearance model* $M_{\widetilde{x}_t}$:

$$\widehat{x}_t = \underset{\widetilde{x}_t \in \mathbb{R}^6}{\operatorname{argmin}} \, f_{obj}(M^*, M_{\widetilde{x}_t}) \tag{1}$$

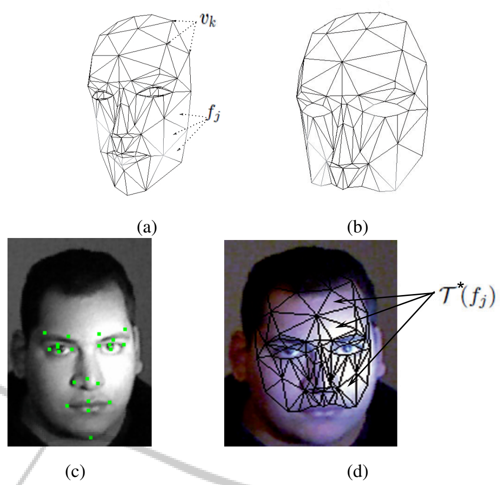

Figure 2: From the Candide model to the reference model M^*. (a) Original Candide model defined as $K = 113$ vertices v_k and $J = 184$ faces f_j. (b) The modified version of the Candide model used in the rigid tracking process containing only $K = 93$ vertices $J = 100$ facets. This version covers only rigid parts of the face. (c) Facial reference points extracted form the image using (Valstar et al., 2010). (d) Texture of the reference model obtained from the color image.

Each of these concepts forming the optimization process will be detailed in the followings sections.

3.1 Reference Model

The reference model M^* used in this work is a textured 3D face model. Without loss of generality we used the Candide model (Ahlberg, 2001). It is defined as a set of K vertices $\mathcal{V}^* = \{v_1, v_2, \ldots, v_K\}$ and a set of J facets $\mathcal{F}^* = \{f_1, f_2, \ldots, f_J\}$ (see figure 2(a)). The initialization of the reference model consist of fitting the Candide deformable model to the user's face by solving the shape variation parameters of the Candide model and extracting its texture by projecting the model in the 2D image of the first acquisition where the face is supposed neutral expression and animation (see (Valstar et al., 2010; Rekik et al., 2013) for more details). First, facial reference points are detected in the color image using (Valstar et al., 2010)(see Figure 2(c)). Using both of the calibration parameters of Kinect and the depth map, one can retrieve 3D coordinates of the detected reference points in the color camera coordinate system. After this fitting step, we keep in the model only facial parts that present the minimum of animation and expression (see Figure 2(b)). The reference texture $\mathcal{T}^*$ is defined by the set of textured facets $\{\mathcal{T}^*(f_1), \mathcal{T}^*(f_2), \ldots, \mathcal{T}^*(f_J)\}$ obtained by projecting the face model on the 2D image (Figure 2(d) shows an example of a reference texture).

3.2 Objective Function and Optimization

The objective function allows the evaluation of a given $\widetilde{x}_t$ by comparing the appearance face model $M_{\widetilde{x}_t}$ to the reference face model M^*. The appearance model $M_{\widetilde{x}_t}$ consists of a set of K vertices $\mathcal{V}_{\widetilde{x}_t}$ and a set of J facets $\mathcal{F}_{\widetilde{x}_t}$. The coordinates of each vertex $\widetilde{v}_k \in \mathcal{V}_{\widetilde{x}_t}$ are computed as follows:

$$\widetilde{v}_k = \mathbf{R}\boldsymbol{v}_k + \mathbf{t} \tag{2}$$

where $\mathbf{R}$ and $\mathbf{t}$ are, respectively, the 3×3 rotation matrix and the translation vector generated in a standard way from the six parameters of $\widetilde{x}_t$. The appearance texture $\mathcal{T}_{\widetilde{x}_t}$ is defined by the set of the textured facets obtained by projecting the transformed face model on the current 2D image.

Our objective function depends on two energies. The first is a geometric energy $E_{geo}\left(\mathcal{V}_{\widetilde{x}_t}, \mathcal{Q}_t\right)$ measuring the closeness of the appearance model on the 3D point cloud $\mathcal{Q}_t$ acquired by the depth sensor of the RGB-D camera in instant t. The second is a photometric energy denoted by $E_{ph}\left(\mathcal{T}^*, \mathcal{T}'_{\widetilde{x}_t}\right)$ where $\mathcal{T}'_{\widetilde{x}_t}$ is the modified appearance texture (will be explained later in section 3.2.2). It indicates the similarity between textures of the reference model and the appearance model $M_{\widetilde{x}_t}$. The combination of these two energies is given by:

$$f_{obj}(M^*, M_{\widetilde{x}_t}) = \alpha\, E_{geo}\left(\mathcal{V}_{\widetilde{x}_t}, \mathcal{Q}_t\right) + (1-\alpha)\, E_{ph}\left(\mathcal{T}^*, \mathcal{T}'_{\widetilde{x}_t}\right) \tag{3}$$

where α is a weighting scalar which we experimentally fixed to 0.8 in our implementation. We refer the reader to (Rekik et al., 2013) for more details about α.

3.2.1 Geometric Energy

The geometric energy indicates the closeness of the appearance model $M_{\widetilde{x}_t}$ to the point cloud $\mathcal{Q}_t$ acquired at a time t and compares their shapes. Given the calibration data of the RGB-D camera, we can define a set of K corresponding points $\{(\widetilde{v}_k, q_k)\}_{k=1}^{K}$ between the vertices $\mathcal{V}_{\widetilde{x}_t}$ of $M_{\widetilde{x}_t}$ and the point cloud $\mathcal{Q}_t$, where $q_k \in \mathcal{Q}_t$, $\widetilde{v}_k \in \mathcal{V}_{\widetilde{x}_t}$, and $q_k$is the closest 3D point to $\widetilde{v}_k$. The geometric energy is defined as the point-plan distance between $\mathcal{V}_{\widetilde{x}_t}$ and $\mathcal{Q}_t$:

$$E_{geo}\left(\mathcal{V}_{\widetilde{x}_t}, \mathcal{Q}_t\right) = \frac{1}{K}\sum_{k=1}^{K} \|n_k^T\left(\widetilde{v}_k - q_k\right)\|^2, \tag{4}$$

where n_k is the surface normal at $\widetilde{v}_k$. In equation 4, more $\mathcal{V}_{\widetilde{x}_t}$ is close to $\mathcal{Q}_t$, more the geometric energy tends toward 0.

3.2.2 Photometric Energy

This energy allows the optimization process to converge toward a face pose with a texture $\mathcal{T}_{\widetilde{x}_t}$ as close as possible to the reference one $\mathcal{T}^*$. The photometric energy is defined as follows:

$$E_{ph}\left(\mathcal{T}^*, \mathcal{T}_{\widetilde{x}_t}\right) = \frac{1}{N}\sum_{p_i^* \in \mathcal{T}^*} \left[\mathcal{T}_{\widetilde{x}_t}\left(w(p_i^*)\right) - \mathcal{T}^*\left(p_i^*\right)\right]^2 \tag{5}$$

where p_i^* is a pixel in $\mathcal{T}^*$, N is the number of pixels in $\mathcal{T}^*$ and $w(p_i^*)$ is a function which compute for each p_i^* its corresponding one in $\mathcal{T}_{\widetilde{x}_t}$. For more details about computing correspondence between pixels in triangular regions see (Maurel, 2008).

Since the image acquired in the instant t can be affected by an arbitrary illumination changes, the photometric energy can give a false assessment. To reduce the effect of changing lighting condition, we propose to use a facial illumination model inspired from (Silveira and Malis, 2007). For face pose tracking, we are interested to solve which lighting variations has to be applied to the current texture $\mathcal{T}_{\widetilde{x}_t}$ in order to obtain a modified texture $\mathcal{T}'_{\widetilde{x}_t}$ whose illumination conditions are as closely as possible to those at the time of initializing $\mathcal{T}^*$. We propose to formulate this problem so as to find an element-wise multiplicative lighting variation $\widetilde{I}$ over the current $\mathcal{T}_{\widetilde{x}_t}$, and a global lighting changes β, such that $\mathcal{T}'_{\widetilde{x}_t}$ matches as closely as possible to $\mathcal{T}^*$:

$$\mathcal{T}'_{\widetilde{x}_t} = \widetilde{I} \circ \mathcal{T}_{\widetilde{x}_t} + \beta \tag{6}$$

where the operator $\circ$ stands for the element-wise product. Since considering that the intensity of each pixel can change independently, we have an observability problem. We suppose that $\widetilde{I}$ is modelled by a parametric surface $\widetilde{I} = f(p_i;\gamma)$, $\forall p_i$, that describes the local illumination variation of each pixel. Vector γ gives the different lighting variation multiplicative values γ_j relative to pixels in a same texture subregion $\mathcal{R}_j$. These texture sub-regions describes the regions in the face for which the illumination variation is linear. Thus, $\widetilde{I}$ reads:

$$\widetilde{I} = f(p_i;\gamma) = \gamma_j, \forall p_i \in \mathcal{R}_j \tag{7}$$

where p_i denotes the i-th pixel of the j-th subregion $\mathcal{R}_j$. In practice, the appearance texture $\mathcal{T}_{\widetilde{x}_t}$ is discretized into n subregions $\mathcal{R}_j, j = 1,2,\ldots,n$, where each $\mathcal{R}_j$ is defined as a set of adjacent triangles in $\mathcal{T}_{\widetilde{x}_t}$. Figure 3 shows an example of discretization of $\mathcal{T}_{\widetilde{x}_t}$ into 4 subregions. Using equation 7, the photometric energy reads:

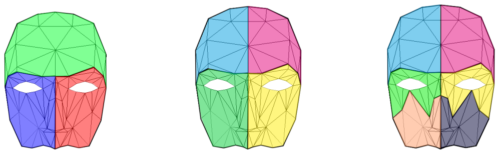

(a) (b) (c)

Figure 3: Different grouping of the face model facets used in the tracking process. (a), (b) and (c) presents, respectively, three, four and six face regions.

$$E_{ph}\left(\mathcal{T}^*,\mathcal{T}'_{\widehat{x}_t}\right)=\frac{1}{N}\sum_{p_i^*\in\mathcal{T}^*}\left[\mathcal{T}'_{\widehat{x}_t}\left(w(p_i^*);\gamma_j,\beta\right)-\mathcal{T}^*\left(p_i^*\right)\right]^2, \quad (8)$$

where p_i^* the i-th pixel of the j-th subregion in $\mathcal{T}^*$ and $\mathcal{T}'_{\widehat{x}_t}(w(p_{ij}^*;\gamma_j,\beta))$ is computed as follows:

$$\mathcal{T}'_{\widehat{x}_t}\left(w(p_i^*);\gamma_j,\beta\right)=\gamma_j\mathcal{T}_{\widehat{x}_t}\left(w(p_i^*)\right)+\beta \quad (9)$$

3.2.3 Optimization

In this study, the minimization of equation 3 is performed using the Nelder-Mead Simplex method (Nelder and Mead, 1965; Press et al., 2007) because of its simplicity and efficiency. The simplex is defined as a convex hull with $6+n+1$ vertices: 6 is the number of the pose parameters, n stands for the face region number (see figure 3) and the last parameter corresponds to β the global illumination changes. The Simplex algorithm is an iterative algorithm starting, in our case, from an initial simplex defined around $\widehat{x}_{t-1}$. Each iteration begins by ordering the current set of vertices according to their evaluation value computed using our objective function. Then, the worst point is discarded and several better trial points are generated and function values are evaluated at these points. A new simplex is then constructed using rules that lead to the minimization of the objective function. The minimization process is stopped when the simplex size is lower than a tolerance value or a maximum number of iteration is reached. The processing rate is about 15 images per second on a standard PC and without multi-threading programming.

4 EXPERIMENTAL EVALUATION

This section details the experiments performed to evaluate our face pose tracking method. First, we evaluate the accuracy of the 3D face pose estimation in normal lighting conditions using the Biwi Kinect Head pose database (Fanelli et al., 2011) which is provided with ground truth data. Then, to demonstrate the robustness of the proposed method to lighting variations, we have used four sequences with severe lighting changes.

4.1 Evaluation on the Biwi Database

The Biwi Kinect Head Pose Database (Fanelli et al., 2011) contains 24 sequences of 24 different persons. In each sequence, a person rotates and translates his face in different orientations. For each frame in the sequences, depth and color images are provided as well as ground truth face poses (3 translations in *mm* and 3 rotation angles in degree).

The evaluation of our tracking method using the Biwi database is done as follows. For a given sequence from the database, we apply our tracking method. Then, we compare the obtained 3D face poses to the ground truth. We define a position error (*i.e.,* Euclidean distance between the obtained face positions and the ground truth ones) and three rotation errors which are the difference between the obtained angles (*i.e.,* yaw, pitch, and roll) and the ground truth angles.

Table 1 shows the mean and standard deviation of error measurements obtained for our method as well as the methods proposed in (Fanelli et al., 2011), (Padeleris et al., 2012) and (Rekik et al., 2013). The second column of table 1 details the position errors and columns 3, 4 and 5 show the estimation errors of the rotation angles *yaw*, *pitch* and *roll* respectively.

From Table 1, we can see that our method is more accurate than the methods proposed in (Fanelli et al., 2011), (Rekik et al., 2013) and (Baltrušaitis et al., 2012). However, our method is as accurate as the one proposed by Pashalis *et al.* (Padeleris et al., 2012) insofar estimation errors presented in (Padeleris et al., 2012) are computed from only 78% of the acquisitions of the Biwi database. Indeed, all acquisitions with location errors and rotations exceeding 10 *mm* and 10°, respectively, were supposed erroneous estimations and ignored in the calculation of the mean and standard deviation of the errors. We note that the standard deviation of the errors is not provided by authors in (Baltrušaitis et al., 2012).

4.2 Robustness Evaluation in Lighting Change Conditions

Since lighting changes in the biwi database sequences is negligible, tracking errors presented in table 1 are not informative about the robustness of the methods in arbitrary lighting change conditions. Consequently, to evaluate the robustness of our method in lighting change conditions, we have recorded four sequences from a Kinect camera for different persons in severe lighting change conditions. To apply nonlinear lighting changes on the face, we have fixed a light source beside the Kinect sensor and the per-

Table 1: Mean and standard deviation of the errors for the 3D face localization and the rotation angles. Errors are computed for all sequences of the Biwi database (Fanelli et al., 2011).

Method	localization (*mm*)	*yaw* (°)	*pitch* (°)	*roll* (°)
Fanelli *et al.* (Fanelli et al., 2011)	14.50 (22.10)	9.10 (13.60)	8.50 (9.90)	8.00 (8.30)
Pashalis *et al.* (Padeleris et al., 2012)	5.21 (2.77)	2.38 (1.80)	2.97 (2.16)	2.75 (2.09)
Tadas *et al.* (Baltrušaitis et al., 2012)	7.56 ( )	6.29 ( )	5.10 ( )	11.29 ( )
Rekik *et al.* (Rekik et al., 2013)	5.10 (3.01)	5.13 (3.33)	4.32 (2.65)	5.24 (3.43)
Our method	5.26 (3.60)	4.21 (1.43)	3.13 (2.40)	4.25 (3.67)

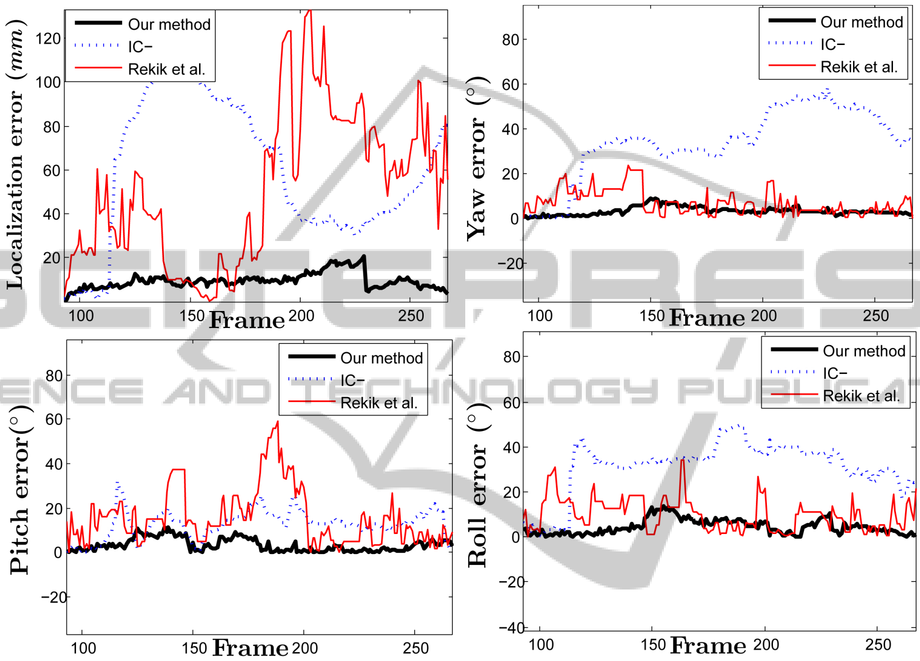

Figure 5: Variation of the localization and the rotation angles errors in the first sequence.

Figure 4: Examples of color images recorded from the RGB camera of the Kinect sensor in different lighting conditions.

son is asked to move his face arbitrary in front of the Kinect camera. Figure 4 shows some frame examples of these sequences.

To provide ground truth to the face pose in each frame, we fit manually the Candide face model to the depth image and its projection to the color image. Ground truths are defined by three translations indicating the nose tip 3D position and three rotation angles (*yaw*, *pitch* and *roll*) indicating the face orientation. Then, we have applied our tracking method for each sequence, and we have computed the tracking error by comparing the obtained 3D face poses to the ground truth ones. Table 2 shows the mean and standard deviation of the errors for the 3D face localization and the rotation angles. The first column in Table 2 shows the tracking errors obtained by the method proposed in (Rekik et al., 2013), while column two and three present the tracking errors of our method without considering illumination change (IC-) and with consideration of illumination change, respectively. Table 2 shows that our tracking method is more robust and accurate since other methods do not handle illumination change in the sequences. Figure 5 shows the variation of the position and the rotation errors obtained by applying the methods presented in table 2 to the first sequence where ground truths are provided only for 180 frames.

Since the number of face regions used for the tracking is important the solve the problem of non-linear lighting changes, we have tested our method with different facet grouping in the face model (see

Table 2: Mean and standard deviation of the errors for the 3D face localization and the rotation angles. Tracking errors are computed from four sequences recorded in changing and severe illumination conditions.

Method	Rekik *et al.*	IC-	Our method
localization (*mm*)	50.50 (36.11)	59.11 (31.26)	9.50 (3.61)
yaw (°)	6.90 (5.59)	33.87 (15.73)	3.17 (1.83)
pitch (°)	15.78 (12.82)	12.52 (6.42)	3.32 (2.93)
roll (°)	9.91 (7.22)	31.15 (11.85)	4.53 (3.32)

Table 3: Variation of the localization and orientation errors according to the number of regions of the face.

Region number	3 regions	4 regions	6 regions
localization (*mm*)	9.50 (3.61)	4.40 (2.40)	3.60 (2.10)
yaw (°)	3.17 (1.83)	2.36 (1.47)	1.18 (0.85)
pitch (°)	3.32 (2.93)	2.87 (2.27)	3.55 (2.94)
roll (°)	4.53 (3.32)	5.86 (3.14)	2.84 (1.87)

figure 3). Then, we have applied our method with the different grouping. Table 3 presents the position and the orientation errors according to the number of regions of the face.

5 CONCLUSIONS

This paper presents a new approach for 3D face pose tracking in illumination condition changes using color and depth data from low-quality RGB-D cameras. Our approach is based on a minimisation process where the objective function combines photometric and geometric energies. We have performed a quantitative evaluation of the proposed method on the Biwi Kinect Head Pose database, and we have demonstrated the robustness of our method in case of arbitrary illumination changes. Future work, will try to ameliorate our tracking speed and will extend our tracker to handle non-rigid facial motions by integrating the Candide facial deformation parameters in the optimization process.

REFERENCES

Ahlberg, J. (2001). Candide-3 - an updated parameterised face. Technical report.

Baltrušaitis, T., Robinson, P., and Morency, L.-P. (2012). 3d constrained local model for rigid and non-rigid facial tracking. In *IEEE CVPR*, pages 2610–2617.

Ben-Hamadou, A., Soussen, C., Daul, C., Blondel, W., and Wolf, D. (2010). Flexible projector calibration for active stereoscopic systems. In *2010 IEEE International Conference on Image Processing*, pages 4241–4244, Hong Kong, Hong Kong.

Ben-Hamadou, A., Soussen, C., Daul, C., Blondel, W., and Wolf, D. (2013). Flexible calibration of structured-light systems projecting point patterns. *Computer Vision and Image Understanding*, 117(10):1468–1481.

Cai, Q., Gallup, D., Zhang, C., and Zhang, Z. (2010). 3d deformable face tracking with a commodity depth camera. In *ECCV*, pages 229–242.

Fanelli, G., Dantone, M., Gall, J., Fossati, A., and Van Gool, L. (2013). Random forests for real time 3d face analysis. *International Journal of Computer Vision*, 101(3):437–458.

Fanelli, G., Weise, T., Gall, J., and Gool, L. V. (2011). Real time head pose estimation from consumer depth cameras. In *IEEE ICPR*, pages 101–110.

Maurel, P. (2008). *Shape gradients, shape warping and medical application to facial expression analysis*. PhD thesis, Ecole Doctorale de Sciences Mathématiques de Paris Centre.

Murphy-Chutorian, E. and Trivedi, M. M. (2009). Head pose estimation in computer vision: A survey. *Pattern Analysis and Machine Intelligence, IEEE Transactions on*, 31(4):607–626.

Nelder, J. A. and Mead, R. (1965). A simplex method for function minimization. *The computer journal*, 7(4):308–313.

Padeleris, P., Zabulis, X., and Argyros, A. A. (2012). Head pose estimation on depth data based on particle swarm optimization. In *IEEE CVPR Workshops*, pages 42–49.

Press, W. H., Teukolsky, S. A., Vetterling, W. T., and Flannery, B. P. (2007). *Numerical recipes: The art of scientific computing*. Cambridge Univ. Press, New York, 3rd edition.

Rekik, A., Ben-Hamadou, A., and Mahdi, W. (2013). 3d face pose tracking using low quality depth cameras. In *VISAPP*, pages 223–228.

Silveira, G. and Malis, E. (2007). Real-time visual tracking under arbitrary illumination changes. In *IEEE CVPR*, pages 1–6.

Smisek, J., Jancosek, M., and Pajdla, T. (2013). 3d with kinect. In *Consumer Depth Cameras for Computer Vision*, pages 3–25. Springer.

Valstar, M. F., Martinez, B., Binefa, X., and Pantic, M. (2010). Facial point detection using boosted regression and graph models. In *IEEE CVPR*, pages 2729–2736.

Yin, L., Wei, X., Longo, P., and Bhuvanesh, A. (2006). Analyzing facial expressions using Intensity-Variant 3D data for human computer interaction. In *IEEE ICPR*, pages 1248–1251.

Zhou, S., Chellappa, R., and Jacobs, D. (2004). Characterization of human faces under illumination variations using rank, integrability, and symmetry constraints. *Computer Vision-ECCV 2004*, pages 588–601.